ELSEVIER

Polymer 40 (1999) 6329–6336

polymer

High density polyethylene as a thermal storage material studied by MAS ^{13}C NMR spectroscopy

O.H. Han[a,*], S.A. Chae[a], S.O. Han[b], S.K. Woo[b]

[a]*Magnetic Resonance Research Group, Korea Basic Science Institute, Yeueundong 52, Yoosung-goo, Taejeon, 305-333, South Korea*
[b]*Energy Materials Research Team, Korea Institute of Energy Research, Taejeon, 305-343, South Korea*

Received 28 April 1998; received in revised form 16 October 1998; accepted 24 November 1998

Abstract

In order to improve the stability of high density polyethylene (HDPE) as a thermal energy storage medium, HDPE was cross-linked by electron beam irradiation. Solid state NMR spectroscopic methods were used to analyze the cross-linked HDPE and its thermal degradation. The influence of ethylene glycol (EG) as a heat transfer fluid on the cross-linked HDPE was also investigated. Neither oxidation nor phase transition was observed in HDPE kept in vacuum, even after 1000 h at 150°C. However, both phenomena were observed in HDPE either kept at 150°C or thermally cycled in air. HDPE completely immersed in EG was not oxidized, but phase transition from crystalline to amorphous, probably caused by the penetration of EG into the HDPE, was detected. The observed increase of amorphous phase was attributed to a result of crystalline to amorphous phase transition of perturbed regions in the crystalline phase close to defect sites occupied by oxidation products or EG molecules.

Keywords: High density polyethylene; ^{13}C NMR; Thermal storage material

1. Introduction

Thermal energy storage plays an important role in the conservation of thermal energy in many processes such as waste heat recovery and load leveling at power plants including those utilizing alternative energy sources [1]. Among several possibilities, high density polyethylene (HDPE) was recommended as a thermal energy storage material because of its large heat of fusion, relatively low cost and congruent melting behavior [2]. HDPE could be made thermally more stable by cross-linking. The cross-linking process does not change HDPE's latent heat. This thermally stable form of HDPE does not require separate packaging, reducing the cost of the thermal energy storage system [3]. Gamma-ray irradiation or chemical reaction was employed to produce cross-links in semi-crystalline polymers [4]. In this work, electron beam irradiation is used to produce cross-links in the HDPE. The electron beam irradiation could result in not only cross-links, but also bond scissions and even oxidization for the HDPE exposed in air during the irradiation. Optimization of the irradiation conditions could be important to minimize undesirable side reactions and to maximize cross-links. Thermal energy storage material degradation is suspected to result mainly from oxidation during repeated thermal cycles. Also, ethylene glycol (EG), a frequently used heat transfer fluid in the thermal energy storage system, may influence the degradation process of HDPE through direct contact with HDPE in our thermal energy storage system.

Polyethylene (PE) has been one of the polymers extensively studied by solid state nuclear magnetic resonance (NMR) [5–22], especially with magic angle spinning (MAS) ^{13}C NMR techniques. Methylene peaks from different phases appear to have different chemical shifts, line widths, and relaxation behaviors [5–12]. Carbons other than methylene carbons contribute negligible intensities in the ^{13}C NMR spectra except in highly oxidized [20], branched [21], or low molecular weight [22] PE. This report is focused on the study of the effect of electron beam irradiation, thermal degradation of the cross-linked HDPE, and the effect of EG on the HDPE with respect to the development of HDPE for a thermal energy storage material with MAS ^{13}C NMR spectroscopy.

2. Experimental

2.1. Sample preparation

HDPE sheets were made from commercial grade HDPE

* Corresponding author. Tel.: + 82 42 865 3436; fax: + 82 42 865 3419.
E-mail address: ohhan@comp.kbsi.re.kr (O.H. Han)

0032-3861/99/$ - see front matter
PII: S0032-3861(98)00835-0

pellets (product number F120A by the Samsung General Chemicals, Korea), without further treatment. The density and melting index of the HDPE pellets were measured as 0.956 g/cm^3 and 0.04 g/10 min, respectively. The melting temperature and the heat of fusion were reported as 124°C and 38.5 cal/g, respectively by the manufacturer. The 1 mm thick sheet was made out of this pellet by molding at 200°C under a pressure of 4.1 kg/cm^2 for 6 min and 54.3 kg/cm^2 for 4 min consecutively.

Electron beam irradiation was carried out on the HDPE sheet with a Samsung-INP Electron Beam Accelerator (Samsung Heavy Industries Co., Ltd., Korea). The HDPE sheet (HP-0) was irradiated with 50, 90, 190 kGy to produce HP-50, HP-90, and HP-190 samples, respectively.

For the thermal degradation studies, a set of HP-0 and HP-90 samples maintained in vacuum were compared with another set of HP-0 and HP-90 samples kept in an air-circulating oven at 150°C for 1000 h. Thermally cycled HP-90 and PEXL (HDPE sample taken from a commercial HDPE ondol[1] pipe manufactured by Samsung) in air were also studied. One thermal cycle is composed of heating at a rate of 30°C/h from room temperature to 150°C, maintaining the temperature for 3 h, and then naturally cooling with the heater off to ambient temperature. For a full thermal cycling experiment, the thermal cycle was applied 400 times to the sample at a rate of 1 cycle/day.

To study the effect of EG on a HDPE energy storage system, HP-90 sheets were completely or partially immersed in EG and maintained at 150°C for 1000 h. Reagent grade EG was purchased from the Oriental Chemical Industries in Korea and used without any further treatment. An air-circulating oven equipped with a thermostat was employed to maintain the temperatures. Gel contents of samples, which could be regarded as contents of cross-linked HDPE, were measured by ASTM D 2765-90 procedure [23]. About 0.3 g of 0.2–0.3 mm thick strips of HDPE was put into xylene. The part of the sample that was undissolved in xylene at 139°C–141°C for 24 h was dried at 150°C for an hour, weighed, and calculated in percentage to the original weight.

Samples processed to sheets by injection method were prepared at 220°C–240°C and 120–130 kg/cm^2 and with a cooling period of about 25 s. Samples processed to sheets by extrusion were prepared at 200°C and 150 kg/cm^2 for 8 min.

2.2. Notation of samples

The following notation will be used in this report for each HDPE sample:

Notation	Meaning
HP-	processed by hot pressing
INJ-	processed by injection
EXT-	processed by extrusion
-#-	HDPE sheet electron beam irradiated with #kGy dosage
-TDO500	kept at 150°C and in air for 500 h
-TDO1000	kept at 150°C and in air for 1000 h
-TDV500	kept at 150°C and in vacuum for 500 h
-TDV1000	kept at 150°C and in vacuum for 1000 h
-EG1000	kept at 150°C and fully immersed in EG for 1000 h
-EG1000 air	kept at 150°C and partially in EG for 1000 h
-cycled	thermally cycled 400 times in air as described in the text
-[powder]	powdered sample
SOLID-upperEG	solidified part at the surface of EG after 1000 h at 150°C when the HDPE was partially exposed to air
PEXL	HDPE taken from a commercial ondol pipe
HP-90-ext	dry gel extracted from HP-90 during ASTM D 2765-90 procedure

For example, INJ-90-TDO500 means the HDPE processed by injection, electron beam irradiated with 90 kGy, and then kept at 150°C and in air for 500 h. Another example is HP-90-cycled-[powder] which is prepared by the hot pressing method, electron beam irradiated with 90 kGy, and then thermally cycled 400 times in air. Then, this sample was powdered before NMR experiments.

2.3. NMR spectroscopy

All NMR experiments were carried out with the UNITY-plus NMR system (Varian Association Inc.) of 7.05 T and a multinuclear cross-polarization magic angle spinning (CPMAS) [24] probe (Varian Association Inc.) at room temperature. Typical spinning rate employed for MAS and CPMAS experiments was 5 kHz. The 90° pulse length for both ^{13}C and ^{1}H was 4.5 μs and proton decoupling strength was 55.6 kHz. All ^{13}C spectra were acquired under proton decoupling, and the ^{13}C chemical shift was referenced to external tetramethyl silane (TMS). Methyl peak of hexamethyl benzene externally set as 17.3 ppm was used as a secondary chemical shift standard [25]. In order to achieve stable spinning, fine NaCl powder was added to fill up the rotor containing packed samples in sheet form. All data were collected using samples in sheet form unless stated otherwise. Some data were taken from the samples powdered at 77 K by a Freezer-Mill (Spex, USA). Simple single contact CP pulse sequence was used with 1500 μs contact time and 5 s pulse sequence repetition delay for CPMAS experiments. For MAS spectra (under proton decoupling but without CP), 4.5 μs pulse length and 1500 s pulse sequence repetition delay were used. Carbon-13 spin–lattice relaxation time (T_{1C}) was measured with Torchia's pulse sequence [26] with 10 s pulse repetition delay.

[1] Korean under-floor heating system.

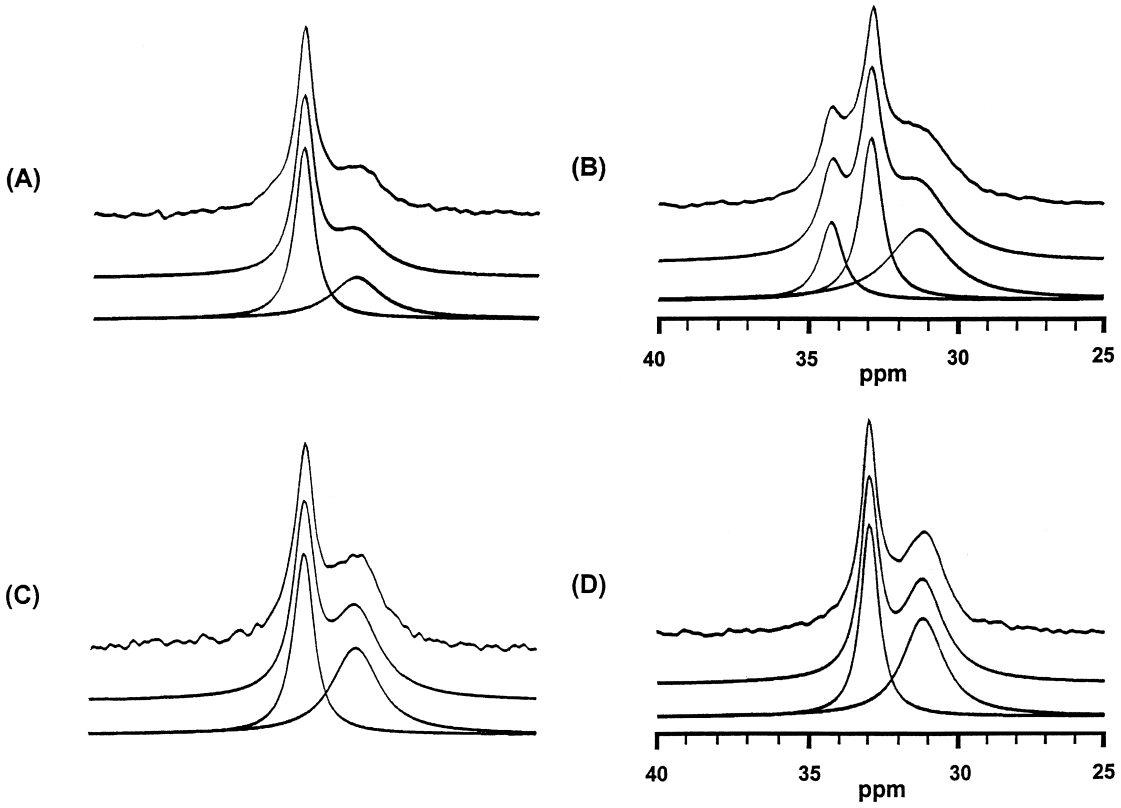

Fig. 1. Carbon-13 MAS spectra of (A) HP-90, (B) HP-90-[powder], (C) HP-90-ext, and (D) PEXL. The top, middle, and bottom parts of each spectrum are the experimental spectrum, the simulated spectrum, and the individual components of the simulated spectrum, respectively. Pulse sequence repetition delay of 1500 s, spinning speed of 5 kHz, line broadening of 15 Hz, and number of acquisition between 12 and 40 were employed.

2.4. Other analytical methods

Differential scanning calorimetry (DSC) (Perkin-Elmer DSC-4, USA) was used to measure melting temperature (T_m) and the heat of fusion (ΔH_f). The measurement was carried out under nitrogen atmosphere, at 10°C/min scan rate, and from 30°C to 200°C for about 10 mg sample. Highly pure indium with $T_m = 156.6$°C and $\Delta H_f = 6.80$ cal/g was used as a standard sample for the DSC measurement. For X-ray diffraction (XRD) experiments, X-ray diffractometer (Rigaku Co., RTP-3000, Japan) with Cu Kα source was employed for the range of $2\theta = 15°–30°$. Fourier Transformation Infrared (FT-IR) spectra were acquired with FT-IR spectrometer (DigiLab Division FTS80, USA) from 400 to 4000 cm^{-1}.

3. Results and discussion

3.1. Interpretation of HDPE ^{13}C NMR Spectra

Representative ^{13}C MAS spectra of our HDPE samples are shown in Fig. 1. Only methylene peaks were recognizable in the spectra, and the peaks at 34.2 ± 0.3, 32.8 ± 0.3, and 31.3 ± 0.3 ppm were assigned to methylene carbons from monoclinic crystalline phase, orthorhombic crystalline phase, and noncrystalline or amorphous phase, respectively. Monoclinic crystalline phase was detectable only in powdered samples. This phenomenon was explained in our previous report [5] as a result of solid–solid phase transition which occurred during powdering process at 77 K. For the peak assignment, peak position, T_{1C}, line width, CP rate, and dipolar dephasing rate of each methylene peak were compared with reported properties [6–10,21]. T_{1C} values from fitting integrated peak areas including all methylene peaks were 180 s and 430 ms for a representative HDPE sample, HP-90. When the peak height at 32.8 ppm was used for fitting, the same T_{1C} values were obtained but the relative population of long component increased. This population change was simply because of the reduced contribution from noncrystalline phase to the peak height at 32.8 ppm compared to the case of integrated peak area measurement; only small tail of the noncrystalline phase peak could contribute to the intensity at 32.8 ppm. Fitting the individual deconvoluted peak areas also resulted in T_{1C} of 180 s for 32.8 ppm peak and 430 ms for 31.3 ppm peak. Therefore, we conclude that crystalline phase has T_{1C} of 180 s and T_{1C} of 430 ms for the noncrystalline phase. Similarly, T_{2C} was calculated from dipolar dephasing data; 0.04 and 1.2 ms were obtained for crystalline and noncrystalline phase, respectively. In an earlier work by Kitamaru et al. [9,10] crystalline-amorphous interfacial component was

Table 1
Relative methylene peak area of ^{13}C MAS spectra and gel content measured by the ASTM D 2765-90

Sample	MCP[a]	OCP[a]	NCP[a]	Gel content (%)
HP-0	0	62	38	0
HP-0-[powder]	17	47	36	0
HP-50	0	58	42	26
HP-90	0	61	39	46
HP-90-[powder]	19	38	43	46
HP-190	0	58	42	65
PEXL	0	50	50	76
PEXL-[powder]	18	35	47	76
HP-90-ext	0	48	52	100
HP-90-ext-[powder]	17	31	52	100
EXT-0	0	61	39	NM[b]
EXT-90	0	60	40	NM
EXT-190	0	62	38	NM
INJ-0	0	59	41	NM
INJ-90	0	59	41	NM
INJ-190	0	59	41	NM
HP-0-TDV1000	0	58	42	NM
HP-50-TDV1000	0	62	38	NM
HP-90-TDV1000	0	60	40	NM
HP-90-EG1000	0	48	48 (EG 4%)[c]	NM

[a] MCP, OCP, and NCP represent monoclinic crystalline phase, orthorhombic crystalline phase, and noncrystalline phase, respectively. All peak areas are described in % and the error range of peak area measurement is within ±3% unless stated otherwise.
[b] Not measured.
[c] Intensity of EG peak at 65 ppm was 4%.

reported. However, our T_{1C} or T_{2C} data did not indicate the presence of interfacial component in our samples. Thus, we simply took the crystalline and noncrystalline phases to assign relaxation data, which was also consistent with the peak assignment by the reported chemical shift values. With powdered samples, we confirmed that both the monoclinic and orthorhombic crystalline phases have the same T_{1C} and T_{2C} relaxation times within the experimental error. The methylene peak areas in the ^{13}C MAS spectra were used to quantify phases in the HDPE samples, and Table 1 summarizes the results.

It is well known that the CP spectra are difficult to quantify because the peak area in the spectra is not linearly proportional to the number of nuclei. However, for the observation of minor components such as oxidation products, methine, or methyl carbons which practically cannot be detected without CP, ^{13}C CPMAS spectra were employed. A referee suggested the use of MAS spectra, obtained without CP but with shorter pulse repetition delay, for example 10–30 s to detect minor components instead of CPMAS spectra. The MAS spectra with shorter pulse repetition delay would result in more accurate population measurement of minor components. However, we found that it took much longer experimental time to get a spectrum than CPMAS method and the spectra obtained by both methods had similar relative peak intensities of minor component except the case that fast moving molecules were

Table 2
Relative peak areas between 20 and 45 ppm of ^{13}C CPMAS spectra

Sample	43.5 ppm	33 ppm (OCP)[a]	30 ppm (NCP)[a]	25 ppm
HP-50-TDV1000	0	77	23	0
HP-90-TDV1000	0	71	29	0
HP-0	0	73	27	0
HP-50	0	72	28	0
HP-90	0	72	28	0
HP-190	0	75	25	0
INJ-0	0	71	29	0
INJ-90	0	75	25	0
INJ-190	0	76	24	0
EXT-0	0	73	27	0
EXT-90	0	75	25	0
EXT-190	0	74	26	0
PEXL	0	60	40	0
HP-0-TDO500	1	54	40	5
HP-0-TDO1000	2	32	52	14
HP-50-TDO500	4	41	47	7
HP-50-TDO1000	2	28	55	16
HP-90-TDO500	4	42	48	5
HP-90-TDO1000	2	30	55	13
HP-190-TDO500	2	36	50	12
HP-190-TDO1000	3	23	51	23
PEXL-cycled	2	22	55	20
HP-90-cycled	4	23	54	19
HP-90-EG1000	0	77	23	0
SOLID-upperEG	2	50	45	3

[a] OCP and NCP represent methylene peaks from orthorhombic crystalline phase and noncrystalline phase, respectively. All peak areas are described in % and the error range of peak area measurement is within ±3% unless stated otherwise.

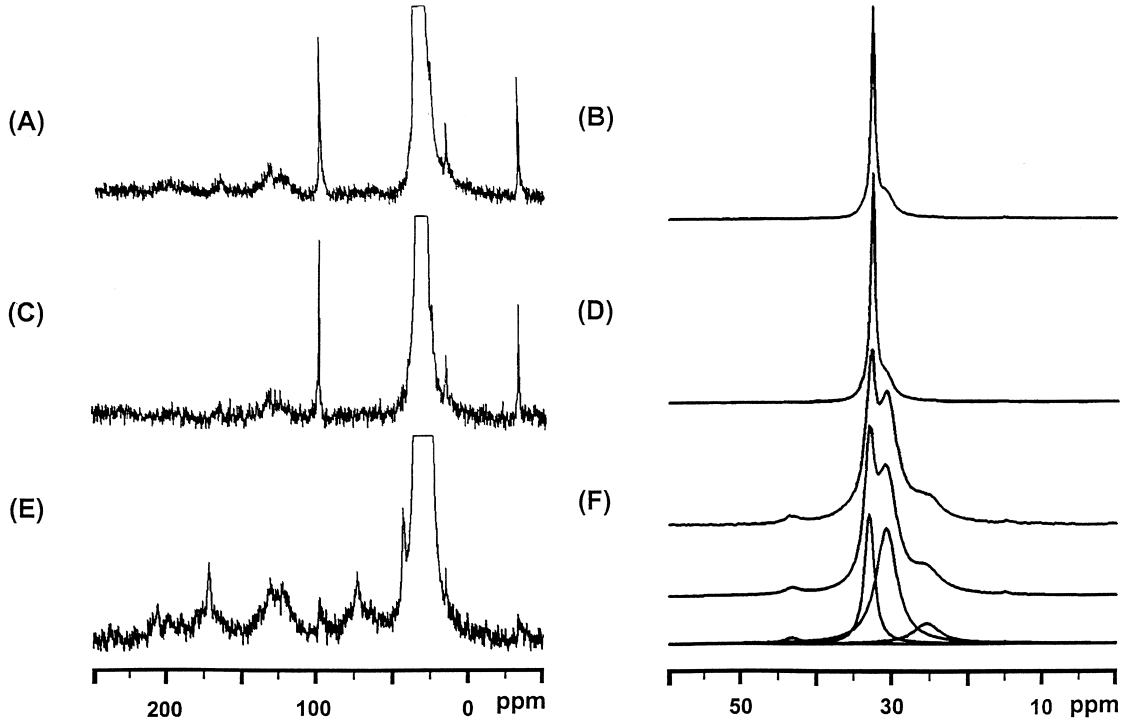

Fig. 2. Carbon-13 CPMAS spectra of HP-90 in (A) and (B), of HP-90-TDV1000 in (C) and (D), and of HP-90-TDO1000 in (E) and (F). The spectra plotted between −50 and 250 ppm were 8 times expanded along *y*-axis in (A), (C), and (E). The spectra in (B), (D), and (F) were plotted from 0 to 60 ppm. Contact time of 1500 μs, repetition time of 5 s, spinning speed of 5 kHz, line broadening of 5 Hz, and the number of acquisition between 1160 and 2802 were employed. The top, middle, and bottom spectra in (F) are the experimental spectrum, the simulated spectrum, and the individual components of the simulated spectrum, respectively.

present in the sample such as EG molecules inside HDPE. Therefore, peak areas of ^{13}C CPMAS spectra, summarized in Table 2, were compared to examine *relative intensity of each peak from different samples*.

Peaks near 100 and −40 ppm in Fig. 2 are spinning side bands of methylene peaks. When the center peak of crystalline methylene carbons has relatively low intensity, its spinning side bands also decrease intensities in Fig. 2(E). There was some contribution of background signal to the humps covering 105–145 ppm, 150–170 ppm, and 175–210 ppm. Therefore, intensities of these humps have little meaning except for the relatively sharp peaks near 75 and 175 ppm in Fig. 2(E). The peak at 75 ppm was assigned to carbons next to oxygen in ether (–C*–O–C*) or next to ester oxygen (–C*–OOC–), and the peak at 175 ppm to carboxylic acid or ester carbons (–C*OO–). If the spectra of *n*-alkanes [22] are referred to, the peak near 15 ppm (the peak near 15 ppm was not clearly seen in Fig. 2(B), (D), and (F) and not included in Table 2 as the peak areas were almost the same for all samples and less than 2–3% close to our error range) should be from methyl carbons, and the peak at 25 ppm should be from methylene carbons next to methyl group. In contrast, referring to the liquid state NMR report [20] on PE oxidation, the peak at 25 ppm should be from beta carbons to carbonyl group, secondary alcohol group, and gamma-lactone, and the peak at 43.5 ppm should be from alpha carbons to corresponding groups. As the intensities of 25 or 43.5 ppm peaks appeared only when the carbonyl peak at 175 ppm is clearly present as shown in Fig. 2(E) and (F), it would be reasonable to assign the peaks at 25 and 43.5 ppm to beta and alpha carbons to the carbonyl groups, respectively, rather than to relate with the methyl groups. There was no recognizable change of the methyl peak intensities among samples even when the intensities of 25 or 43.5 ppm peaks were changed dramatically. This also suggests that 25 and 43.5 ppm peaks are not from alpha or beta carbons to methyl groups. Error range for the peak area measurement was within ±3%, including NMR experimental error, as well as deconvolution error, unless stated otherwise.

3.2. Difference of processing methods to make HDPE sheets

HDPE sheets prepared by hot pressing, injection, or extrusion processing method were compared, but did not show any difference in ^{13}C NMR spectra within experimental error. They all have 60% ± 3% and 40% ± 3% relative peak area for crystalline and noncrystalline phase methylene peak, respectively, in the MAS spectra as summarized in Table 1. There were no noticeable peaks of oxidation products in CPMAS spectra either. All CPMAS spectra were the same as in Fig. 2(A) and (B).

3.3. Cross-links in HDPE by electron beam irradiation

Gel contents of some HDPE were measured by the ASTM D 2765-90 as summarized in Table 1. Although the gel content of electron beam irradiated HDPE such as HP-50, HP-90, and HP-190 appeared to be up to 26%, 46%, and 65%, respectively, there were little changes between HP-0, HP-50, HP-90, and HP-190 in the results of DSC, XRD, and ^{13}C NMR experiments. For example, the melting temperature and the heat of fusion of HP-90 ($T_m = 124$°C, $\Delta H_f =$ 161 J/g) measured with DSC were the same as those of HP-0 within experimental error. Also, the cross-linked HDPE showed the characteristics of the heat charge/discharge performance as a thermal energy storage material. From the results of ^{13}C MAS NMR, the crystalline and noncrystalline phase were found to be 60% ± 3% and 40% ± 3% in fraction, respectively, for all HP-0, HP-50, HP-90, and HP-190 within experimental error. Compared with the CPMAS spectrum of HP-0, no new peaks were noticeable in the CPMAS spectra of HP-50, HP-90, and HP-190. This result indicates that if oxidation or chemical bond scission occurs during irradiation, their products are below the detection limit of ^{13}C CPMAS NMR techniques.

It may be concluded from the results of HP-90-ext and PEXL that in general, noncrystalline phase methylene peak area in the ^{13}C MAS spectra of highly cross-linked HDPE is larger than that for less cross-linked HDPE. The gel extracted from HP-9 [denoted as HP-9-ext], which can be regarded as 100% cross-linked HDPE, has 52% ± 3% noncrystalline component from methylene NMR peak area measurement of ^{13}C MAS spectra. The PEXL which is supposed to be cross-linked more than 75% has 47% ± 3% noncrystalline component from methylene peak area measurement. The reason why noncrystalline components of HP-0, HP-50, HP-90, and HP-190 samples are the same within the experimental error though they have different cross-link contents is probably because of the fact that the variation of noncrystalline components is within the experimental error range (±3%). Compared with the CPMAS spectrum of HP-0, no new peaks were noticeable in the CPMAS spectra of PEXL and HP-90-ext. Therefore, it could be deduced that a greater amount of noncrystalline component was induced mainly by more cross-links, and not by oxidation or chemical bond scission in HDPE. No increase of the noncrystalline component by cross-linking in HP-50, HP-90, and HP-190 was observed, possibly because cross-links in them were not enough to influence noncrystalline component content. When the amount of cross-linked HDPE in the sample (gel content in Table 2) is smaller than or equal to 65%, the variation of noncrystalline phase methylene peak area might be ±3% at most, which corresponds to the error range of detection by NMR. However, this deduction needs some caution to be declared as HP-90-ext underwent an extra procedure which could cause phase transitions. HP-90-ext was solidified from gel. PEXL was prepared from HDPE different from our HDPE pellets and cross-linked by an unknown method to us. Thus, there is a possibility that the PEXL might have more than 40% of noncrystalline phase methylene peak area even before cross-linking. This makes it difficult to compare both the PEXL and HP-90-ext with HDPE cross-linked by electron beam irradiation such as HP-50, HP-90, and HP-190. Thus, we conclude tentatively that the noncrystalline phase methylene peak area is not affected by the content of cross-links created by electron beam irradiation.

3.4. Thermal degradation of HDPE

Phase change and oxidation of HDPE were observed after thermal degradation in air at 150°C for 1000 h. HP-90-TDO1000 sample did not show any endotherm peaks in the range of 50°C–200°C. In contrast, no peak difference in the DSC plots was detected between the HP-90-TDV1000 and the original HP-90 kept at room temperature. The typical crystalline XRD peaks of HP-90 were easily observed in the HP-90-TDV1000, whereas they were not detected in the HP-90-TDO1000. The HP-90-TDV1000 and the HP-90 showed the same ^{13}C CPMAS NMR spectra, while the HP-90-TDO1000 showed increased noncrystalline component and more oxidation products (Fig. 2).

For our thermal degradation study, ^{13}C CPMAS NMR spectra were taken instead of ^{13}C MAS NMR spectra, and relative intensity variation of each peak among different samples was observed; this value is summarized in Table 2. Thermally degraded HDPE, such as HP-90-TDO1000 and HP-90-cycled, did not have enough crystalline phase methylene peak area to be accurately measured and compared with noncrystalline phase methylene peak area in ^{13}C MAS NMR spectra. In addition, small peaks from oxidized products such as the ones at 175, 75, 43.5 and 25 ppm in the ^{13}C CPMAS NMR spectra of the HP-90-TDO1000 in Fig. 2(E) and (F) were not observed in ^{13}C MAS NMR spectra.

The HP-90-TDO1000 had a broader band near 3000–3600 cm^{-1} and a new band at 1600–1750 cm^{-1} in the FT-IR spectra. The broader band appeared to be because of the the larger number of terminal hydroxyl groups, and the new band at 1600–1750 cm^{-1} is assigned to the carbonyl stretching vibration. This result confirms that new products which have carbonyl groups are produced during the thermal degradation process, agreeing with the NMR results.

As seen in Table 2, the crystalline phase appeared to be partially transformed to the noncrystalline phase as a result of the thermal degradation in air. The greater amount of noncrystalline phase methylene peak area in the MAS and CPMAS spectra of oxidized samples could be because of the crystalline to noncrystalline phase transition of perturbed regions in the crystalline phase next to the oxidation products. Interestingly, HDPE irradiated with a higher dosage (HP-190-TDO1000) has smaller relative crystalline phase methylene peak area and greater 25 ppm peak area than the HDPE irradiated with

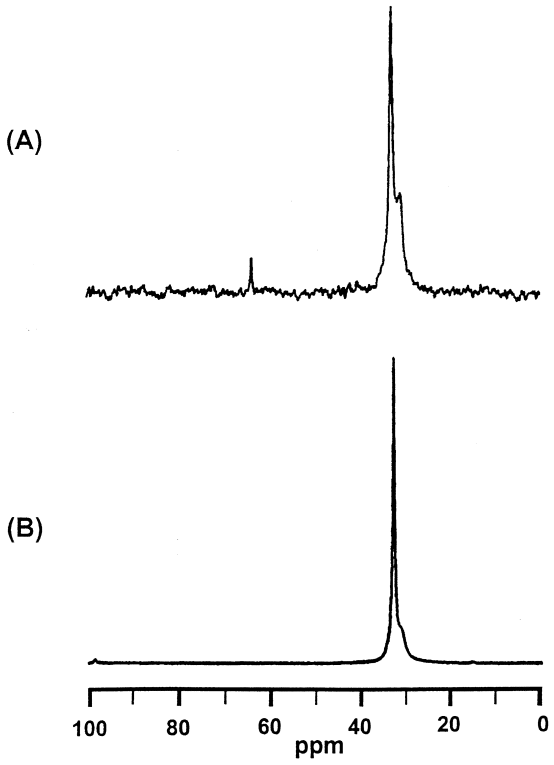

Fig. 3. Carbon-13 (A) MAS and (B) CPMAS spectra of HP-90-EG1000. Spinning rate was 5 kHz. Pulse repetition delay of 1500 s, 24 scans, and line broadening of 15 Hz were used for the MAS spectrum. Pulse repetition delay of 5 s, contact time of 1500 μs, 1600 scans, and line broadening of 1 Hz were used for the CPMAS spectrum.

lesser dosage (HP-90-TDO1000 or HP-50-TDO1000) or unirradiated HDPE (HP-0-TDO1000) after 1000 h at 150°C and in air. These results imply that the HDPE irradiated with higher dosages are more susceptible to oxidation in air. It was also noticed that the thermally cycled sample (HP-90-cycled) was more oxidized and had lesser crystalline phase left than HP-90-TDO1000. These results suggest that electron beam irradiation with a 90 kGy dosage produced HDPE that was mechanically more stable and less oxidized than HDPE unirradiated or irradiated with different dosages. Unless the HDPE is exposed to air, HP-90 is stable and not degraded even after prolonged use at 150°C.

3.5. Effect of EG as a heat transfer liquid on HDPE

EG was frequently used as a heat transfer fluid in the thermal energy storage system. In our thermal storage system, EG and HDPE directly contact each other, and the heat transfer between HDPE and EG occurs on the surface of HDPE. It was found that HP-90 was stable when it was immersed completely in EG even at 150°C for 1000 h (HP-90-EG1000). The ^{13}C MAS NMR spectrum of the HP-90-EG1000 (Fig. 3(A)) was similar to that of the HP-90 before any thermal treatment except for the EG peak at 65 ppm, which had about 4% intensity of the total carbon signal (Table 1). The peak at 65 ppm was from EG molecules inside the HP-90-EG1000 sheet. The sample was rinsed with distilled water for seven days to remove surface adsorbed EG before NMR experiments, but the EG peak was still observable. In contrast, the CPMAS spectrum of the HP-90-EG1000 (Fig. 3(B)) showed no EG peak, which implies that EG molecules are moving around fast enough not to be cross-polarized. When EG molecules penetrated into the HP-90-EG1000 sample, the noncrystalline phase methylene peak area became greater in Table 1 even though oxidation had not progressed. This observation can be attributed to perturbation in the crystalline phase by EG molecules in it resulting in phase transformation from crystalline to noncrystalline phase, though the perturbation was much smaller than that by oxidation.

The HP-90 in EG that was partially exposed to air at 150° for 1000 h (HP-90-EG1000air) underwent similar thermal degradation to the thermally degraded samples in air, resulting in increased noncrystalline phase and more oxidation products (Table 2). When the HP-90 in EG was partially exposed to air, some HDPE and its oxidation products were solidified on the surface of EG after the thermal degradation at 150°C for 1000 h. The solidified part (SOLID-upperEG) had qualitatively the same ^{13}C NMR spectra as those of thermally degradaded HDPE such as HP-90-TDO1000 (Table 2).

In the spectrum of the EG used for the preparation of HP-90-EG1000 (Fig. 4(A)), peaks from oxidation products were observed; no peak from PE was observed. We assigned the peaks at 176, 165, and 164 ppm to carbonyl groups. The carbonyl carbons was up to 0.4% of total carbons in the EG sample from ^{13}C intensity measurement. These oxidation products were confirmed to be products of EG rather than of HDPE by the fact that the HDPE fully immersed in EG was not oxidized at all while the EG in the same system was. In addition, the virgin EG sample has no carbonyl peak in its ^{13}C NMR (Fig. 4(B)), but the spectrum of EG alone kept at 150°C for 560 h (Fig. 4(C)) did. Thus, the HDPE fully immersed in EG was not oxidized at all even when the EG in the same thermal bath was. The HDPE was not dissolved into EG at all. In contrast, when the HDPE in EG was partially exposed to air, some portion of PE as well as its oxidation products smeared out to EG and was solidified at the upper part of EG.

4. Conclusion

HDPE was cross-linked by the electron beam irradiation for the purpose of developing a thermal energy storage material that would not require separate packaging. The electron beam irradiated HDPE showed characteristics of charge/discharge performance as a thermal storage material. The cross-linked HDPE showed thermal stability even at 150°C if it was not exposed to air. Properties of HDPE, such as melting temperature, heat of fusion, and crystallinity, were not noticeably changed by the electron beam

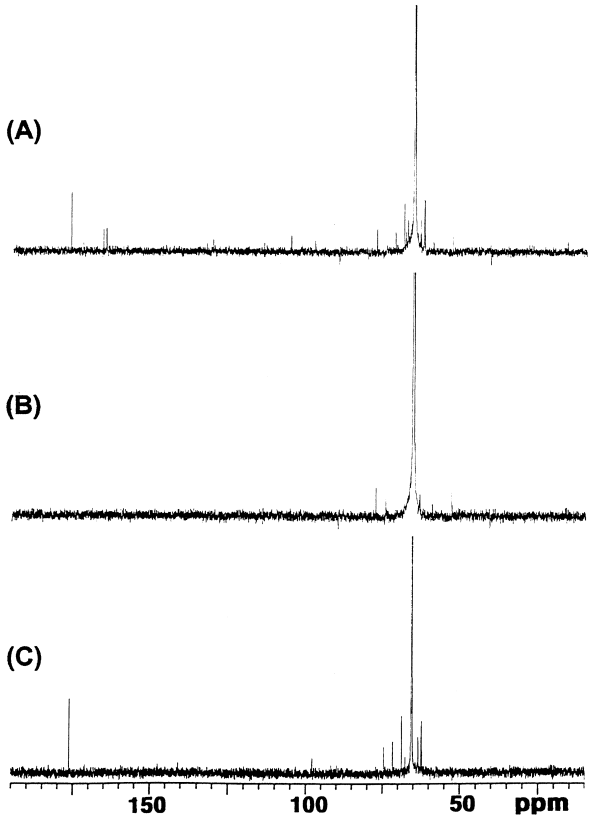

Fig. 4. Carbon-13 NMR spectra of (A) EG used for the preparation of HP-90-EG1000 sample, (B) virgin EG, and (C) EG kept at 150°C and in air for 560 h. 2048 scans, 30 deg pulse of 2.7 μs, pulse repetition delay of 5 s, and line broadening of 1 Hz were employed for each spectrum. D_2O of about 10% in volume was added for deuterium lock.

irradiation. Neither were the HDPE's orthorhombic crystalline and noncrystalline phases.

Thermal degradation was observed as oxidation products such as carboxylic acid and ester groups and as the increased noncrystalline phase content of the samples exposed to air. Degradation was the worst for the HDPE irradiated with 190 kGy and was the least over all for the HDPE irradiated with 90 kGy. However, the samples kept in vacuum did not show any degradation even after 1000 h at 150°C. The sample immersed completely in EG shows no trace of oxidation, but the amount of noncrystalline phase was increased slightly because of the EG molecules penetrating the HDPE. The increase of noncrystalline phase methylene intensity was interpreted as a result of crystalline to noncrystalline phase transition of perturbed regions in the crystalline phase next to defect sites occupied by oxidation products or EG molecules.

In summary, HDPE cross-linked by electron beam irradiation was proved to be an economic thermal energy storage material, as long as it is used in an environment without oxygen.

Acknowledgements

This work was supported partly by a grant (KOYOU project) from the Ministry of Science and Technology (MOST), the Republic of Korea.

References

[1] Lane GA. Solar energy storage; latent heat materials. Technology, vol. 2. New York: CRC Press, 1986.
[2] Salyer IO, Davison JE. J Appl Polym Sci 1983;28:2903.
[3] Whitaker RB, Craven SM, Etter DE, Jendrek EF, Nease AB. Ind Eng Chem Prod Res Dev 1983;22:657.
[4] Mathias LJ, editor. Solid state NMR of polymers. New York: Plenum Press, 1991, chapters 5 and 6.
[5] Han OH, Chae SA, Han S, Woo S. Bull Korean Chem Soc 1996;17:1074 and references therein.
[6] Schroter B, Posern A. Makromol Chem 1981;182:675.
[7] Earl W, VanderHart DL. Macromolecules 1979;12:762.
[8] VanderHart DL, Khoury F. Polymer 1984;25:1589.
[9] Kitamaru R, Horii F, Murayama K. Macromolecules 1986;19:636.
[10] Kitamaru R, Horii F, Zhu Q, Bassett DC, Olley RH. Polymer 1994;35:1171.
[11] Jarrett WL, Mathias LJ, Porter RS. Macromolecules 1990;23:5164.
[12] Tzou DL, Schmidt-Rohr K, Spiess HW. Polymer 1994;22:4728.
[13] Axelson DE, Mandelkern L, Popli R, Mathieu P. J Polym Sci Polym Phys Ed 1983;21:2319.
[14] VanderHart DL, Garroway AN. J Chem Phys 1979;71:2773.
[15] VanderHart DL. Macromolecules 1979;12:1232.
[16] Morin FG, Delmas G, Gilson DFR. Macromolecules 1995;28:3248.
[17] Shimizu Y, Harashina Y, Sugiura Y, Matsuo M. Macromolecules 1995;28:6889.
[18] Chen W, Fu Y, Wunderlich B, Cheng J. J Polym Sci Polym Phys Ed 1994;32:2661.
[19] Tzou DL, Huang TH, Desai P, Abhiraman AS. J Polym Sci Polym Phys Ed 1993;31:1005.
[20] Cheng HN, Schilling FC, Bovey FA. Macromolecules 1976;9:363.
[21] Laupretre F, Monnerie L, Barthelemy L, Vairon JP, Sauzeau A, Roussei D. Poly Bull 1986;15:159.
[22] VanderHart DL. J Magn Res 1981;44: 117.
[23] ASTM D2765-90. Standard test method for determination of gel content and swell ratio of crosslinked ethylene plastics.
[24] Grimmer A-R, Blumich B. In: Diehl P, Fluck E, Gunther H, Kosfeld R, Seelig J, editors. Solid-state NMR I: methods. Berlin: Springer, 1994, chapter 1.
[25] System operation manual VNMR 4.3 Pub. No. 87-195100-00 Rev. G0993, Varian NMR Instruments, Palo Alto, 1993, p. 340.
[26] Torchia DA. J Magn Res 1978;30:631.